



# Inhibition of Induced Chemoresistance by Cotreatment with BVDU

## Inhibition of Induced Chemoresistance by Cotreatment with (E)-5-(2-Bromovinyl)-2'-Deoxyuridine (RP101)

**Rudolf Fahrig, Jörg-Christian Heinrich, Bernd Nickel, Falk Wilfert, Christina Leisser, Georg Krupitza, Christian Praha, Denise Sonntag, Beate Fiedler, Harry Scherthan and Heinrich Ernst**

RESprotect, Dresden, Germany D-01307 [R. F., J-C. H., F. W., C. P., D. S.]; Baxter Oncology, Frankfurt am Main, Germany 60314 [B. N.]; Institute of Clinical Pathology, University of Vienna, Vienna, Austria 1097 [C. L., G. K.]; Medical School Hannover, Hannover, Germany 30625 [B. F.]; Max-Planck-Institute for Molecular Genetics, Berlin, Germany 14195 [H. S.]; and Fraunhofer Institute for Toxicology and Experimental Medicine, Hannover, Germany 30625 [H. E.]

### Abstract

Induced chemoresistance leads to the reduction of apoptotic responses. Although several drugs are in development that circumvent or decrease existing chemoresistance, none has the potential to prevent or reduce its induction. Here, we present data from a drug that could perhaps fill this gap. Cotreatment of chemotherapy with (E)-5-(2-bromovinyl)-2'-deoxyuridine (BVDU, RP101) prevented the decrease of apoptotic effects during the course of chemotherapy and reduced nonspecific toxicity. Amplification of chemoresistance genes (*Mdr1* and *Dhfr*) and overexpression of gene products involved in proliferation (DDX1) or DNA repair (UBE2N and APEX) were inhibited, whereas activity of NAD(P)H: quinone oxidoreductase 1 (NQO1) was enhanced. During recovery, when treatment was with BVDU only, microfilament proteins were up-regulated, and proteins involved in ATP generation or cell survival (STAT3 and JUN-D) were down-regulated. That way, in three different rat tumor models, the antitumor efficiency of chemotherapy was optimized, and toxic side effects were reduced. Because of these beneficial properties of BVDU, a clinical pilot Phase I/II study with five human tumor entities has been started at the University of Dresden (Dresden, Germany). So far, no unwanted side effects have been observed.



## Introduction

Repeated chemotherapeutic treatment frequently induces, or selects for, chemoresistance of remaining cancer cells by altering gene expression and inducing genomic instability because of mutation, recombination, and gene amplification events. Deregulation of DNA-repair enzymes is partly involved in this phenomenon (e.g. *p53* gene, *BRCA1/2*, *UBE2N*, *APEX*, and *Rad51*). Furthermore, enzymes that metabolize and bioactivate drugs [e.g. dihydrofolate reductase (DHFR) (1) and NQO1 (2)] or proteins that transport cytotoxic agents (e.g. multidrug resistance protein (MDR1, Ref. 3]) often contribute to chemoresistance.

During the implementation of a long-term screening program for inhibitors of chemoresistance, BVDU (3) was the only substance of clinical relevance we identified. It inhibited 2-amino-6-mercaptapurine-induced SV40 amplification (4) in Chinese hamster cells, and abrogated triethylene-melamine-induced recombination in yeast (5). In Friend mouse erythroleukemia cells, treatment with DOX induced *Mdr1* gene amplification and drug resistance, which was prevented by simultaneous treatment with BVDU (6). Because the mode of action of BVDU in respect to these effects is unknown, this study aimed to elucidate underlying mechanisms. The preclinical data we obtained were a prerequisite for the start of clinical trials.

We performed *in vitro* experiments with AH13r rat hepatosarcoma and mouse 3T6 cells, and *in vivo* experiments with DMBA-induced SD-rat fibrosarcomas and adenocarcinomas. To test BVDU in a second *in vivo* cancer model, we injected AH13r cells into SD-rats for tumor induction.

As most antineoplastic drugs eliminate tumor cells by apoptosis, cancer cells can evade cell death by virtue of overactivated survival mechanisms. Thus, chemoresistance mechanisms can involve antiapoptotic traits. Therefore, we investigated several survival mechanisms, as well as the activated STAT3, and JUN-D. Moreover, we tested the activity of NQO1, an activating enzyme for anticancer drugs like MMC, MXA, or DOX, which is down-regulated in multidrug-resistant AH130 tumor cells. To identify a more comprehensive spectrum of BVDU-influenced proteins, we performed a two-dimensional gel electrophoresis and identified proteins that are differentially expressed in response to BVDU using MALDI-MS.



## Materials and Method

### Chemicals.

DMBA, MMC, MTX, and DOX were from Sigma (Deisenhofen, Germany). MXA, cisplatin, glufosfamide, and DOX for *in vivo* tests were from Asta Medica (Frankfurt am Main, Germany). BVDU (RP101) was from RESprotect and Berlin-Chemie (Berlin, Germany). RNase was from Boehringer (Mannheim, Germany), and restriction enzymes were from New England Biolabs (Schwabach, Germany). All of the other chemicals were purchased from Sigma and Roth (Karlsruhe, Germany).

### 3T6 Cell Culture and Development of Methotrexate Resistance.

Swiss albino mouse fibroblasts, 3T6, were grown in DMEM supplemented with 10% fetal bovine serum, penicillin, and streptomycin (Biochrom, Berlin, Germany). Cells ( $2.8 \times 10^5$ ) were plated into 9 T25-flasks with MTX, and 9 T25-flasks with MTX and 30  $\mu\text{M}$  BVDU. As soon as cells approached confluency, they were trypsinized and replated at the next higher drug concentration. The MTX concentration was increased 1.5-fold at 1-week intervals for 60 days starting with 44 nM MTX. The number of living cells was determined using the Cell Counter and Analyser System CASY TT (Schärfe System GmbH, Reutlingen, Germany). Cell counting and cell volume determination were hereby based on the displacement of conductive electrolyte by dielectric cells. The signals generated by the cells suspended in an electrolyte were evaluated by pulse area analysis. The pulse area of the signal was strictly proportional to the volume of the particle generating the signal. In dead cells, the integrity of the cell membrane is lost. This loss increased the conductivity and reduced the pulse area of the electric signal. Thus, to exclude debris and dead cells, only particles with a size of  $>7.5 \mu\text{m}$  were counted as cells.

### Treatment of AH13r Sarcoma Cells in Culture.

AH13r cells, a subline of the rat Yoshida sarcoma, were obtained from the Cell and Tumor Bank of the West German Cancer Center, University Essen, Medical School (Essen, Germany). Cells were grown in DMEM (FG 0415; Biochrom AG, Berlin, Germany) supplemented with 10% (v/v) heat-inactivated fetal bovine serum, 100 units/ml penicillin, and 100  $\mu\text{g}/\text{ml}$  streptomycin in a humidified atmosphere containing 5%  $\text{CO}_2$  at 37°C. Logarithmically growing cells were seeded at a density of 100,000 cells/ml and incubated with different cytostatic drugs in combination with or without BVDU. After 2–4 days (unless otherwise indicated), cells were counted using the Cell Counter and Analyser System CASY TT (Schärfe System GmbH), and serially passaged.

### HOP1 Double Staining.

Apoptosis was assayed by HOP1 staining as described by Gruschet *et al.*. Viable, apoptotic, and necrotic cells were counted. The Hoechst 33258 dye stains the nuclei of all cells. Nuclear changes associated with apoptosis, such as chromatin condensation and nuclear fragmentation, can be readily monitored and quantified. Propidium iodide uptake indicates loss of membrane integrity characteristic for necrotic and late apoptotic cells. The selective uptake of the two dyes allows to distinguish between apoptotic and necrotic cell death. Necrosis is characterized in this system by nuclear propidium iodide uptake into cells without chromatin condensation or nuclear fragmentation.



#### **Treatment of AH13r Sarcomas in SD-Rats.**

Ten SD-rats per treatment group were given a single s.c. injection of ascites Yoshida AH13r hepatoma cells. Five to 7 days after tumor application, the growth of the resulting tumors (at the injection site) was suppressed by i.p. treatment of the animals with 2 or 4 mg/kg DOX (9 times within 3 weeks), 120 or 140 mg/kg lufosfamide (15 times within 3 weeks), and 0.5 or 1.5 mg/kg cisplatin only (4 or 5 times within 3 weeks), and by additional oral treatment with 15 mg/kg BVDU (15 times within 3 weeks).

#### **Treatment of DMBA-induced Fibrosarcomas and Mammary Adenocarcinomas in SD-Rats.**

SD-rats (3.5 weeks old) were purchased from Harlan Winkelmann (Borchen, Germany). The care and use of the animals were in accordance with institutional guidelines.

At an age of 39 days, a total of 8 male and 8 female rats were administered s.c. 10 mg DMBA in 0.75 ml sesame oil (DAB 10) to induce fibrosarcomas at the injection site (neck) and (multiple) mammary adenocarcinomas in female rats. DMBA induces mammary tumors that are comparable with those in humans in terms of their long relative latency, histotypes, and endocrine responsiveness (12).

#### **Treatment with DOX or DOX + BVDU.**

Beginning at an age of 128 days, 2 male and 2 female rats were administered three times a week for 8 weeks s.c. with 1 mg/kg DOX (in 0.9% NaCl solution). Another 3 male and 3 female rats were administered three times a week for 8 weeks s.c. with 1 mg/kg DOX and five times a week p.o. with 15 mg/kg BVDU (in corn oil). The control group of 3 male and 3 female rats received 1 ml of a 0.9% NaCl solution i.p., and 5 ml corn oil p.o. five times a week.

#### **Determining Tumor Incidences.**

The rats were checked for tumors by palpation regularly twice a week. The rats were killed when the detectable tumor burden did not allow longer treatment. The surviving animals were killed 60 days after beginning the administration of DOX or DOX+BVDU. An autopsy was performed, and tumor samples were fixed in 10% formalin. All of the tumors were embedded in paraffin, sectioned at 4  $\mu$ m, stained with H&E, and examined histologically. Another sample of each tumor was snap-frozen in liquid nitrogen for additional analysis.

#### **Southern Blot Analysis.**

Analyses were performed using standard procedures (13).

#### **Western Blot Analysis.**

Pelleted cells were suspended in buffer A (20 mM HEPES, 400 mM NaCl, 25% v/v glycerol, 1 mM EDTA, 0.5 mM NaF, 0.5 mM Na<sub>3</sub>VO<sub>4</sub>, and 0.5 mM DTT) according to Pagano *et al.* (14), supplemented with Complete Protease Inhibitor Tablets (Roche, Mannheim, Germany) as described by the manufacturer and then shock-frozen in liquid nitrogen, thawed on ice, and centrifuged (15 min, 4°C, 11,500 rpm). The concentration of protein in the supernatant was determined by the Bradford method using bovine

7



-globulin as a standard (Bio-Rad, Munich, Germany).

SDS-PAGE was performed on a 12% polyacrylamide gel with 10 µg of total protein per lane. Proteins were transferred to a polyvinylidene difluoride membrane (Amersham, Freiburg, Germany) using the Mini *trans*-Blot apparatus (Bio-Rad) with transfer buffer (25 mM Tris base, 192 mM glycine, and 15% v/v methanol) for 4 h at 50 V on ice. Consistent protein loadings and transfer efficiency were verified by Ponceau S-staining.

Destained membranes were blocked with 5% nonfat dry milk in TBST-buffer (20 mM Tris base, 137 mM NaCl, and 0.1% v/v Tween 20) followed by incubation with the respective antibodies overnight at 4°C. Antibody dilutions were as follows: cleaved caspase-3 (Asp175) antibody (Cell Signaling Technology) 1:2000 in blocking buffer, STAT3 (NEB, Frankfurt a.M., Germany) 1:500, JUN-D (Santa Cruz Biotechnology, Santa Cruz, CA) 1:1000, and anti-P-glycoprotein antibody (Alexis, Grünberg, Germany) 1:3000–1:4000.

After washing, blots were incubated with secondary antibody-horseradish peroxidase conjugates, washed again, and protein bands were visualized using chemiluminescence reagent plus (NEN, Boston, MA). Images were captured with a Kodak Image Station 440CF and analyzed with 1d Image Analysis Software (version 3.5; Kodak).



### **CGH.**

DNA labeling and CGH on normal rat chromosomes obtained from fetal rats were performed as described previously (15). Briefly, equal amounts of digoxigenin- and biotin-labeled genomic DNA from drug-treated and from BVDU + drug-treated tumors, respectively, were hybridized to normal metaphases obtained from fetal rat cells. Hybrid molecules were detected with one layer of avidin-FITC (Sigma, Munich, Germany) and rhodamine-antidigoxigenin Fab fragments (Roche Diagnostics, Mannheim, Germany). Slides were mounted and counterstained with antifade solution containing 1 µg/ml 4,6-diamidino-2-phenylindole and actinomycin D (both Serva, Heidelberg, Germany) and analyzed using a cooled CCD camera (Hamamatsu Photonics, Herrsching, Germany) mounted on a Zeiss Axioskop epifluorescence microscope (Carl Zeiss, Göttingen, Germany). The ISIS Digital Image Analysis System (MetaSystems, Altlußheim, Germany) was used for ratio profile analysis, which was based on >7 well-hybridized metaphases.

### **Real-Time PCR.**

Genomic DNA was isolated from each cell subline at various time points using the DNeasy Tissue kit (Qiagen, Hilden, Germany) in accordance with the manufacturer's instructions. Real-time PCR was performed using the ABI Prism 7700 Sequence Detection System (Applied Biosystems, Foster City, CA). For the target gene, *Dhfr*, amplification mixes (30 µl) contained 0.8 ng genomic DNA, 10x SYBR-Green buffer, 200 µM dATP, dCTP, dGTP, and 400 µM dUTP, 3 mM MgCl<sub>2</sub>, 0.75 units of AmpliTaqGold, 0.3 units of AmpErase uracil *N*-glycosylase (Applied Biosystems), and 200 nM of each primer (Thermo Hybaid, Ulm, Germany). For the reference gene, 18S rRNA, 10x TaqMan buffer, 5 mM MgCl<sub>2</sub>, 400 nM of each primer, and 200 nM TaqMan fluorogenic probe (Thermo Hybaid) were used. Thermal cycling consisted of 40 cycles at 95°C for 15 s and 60°C for 1 min, and contained an initial step of 2 min at 50°C and 10 min at 95°C. We prepared a reference calibration curve with stepwise dilutions (1:5) starting with 100 ng genomic DNA. Each 96-well microplate included the standard curve and the sample genomic DNA in triplicate. The normalized *Dhfr* gene copy number was derived from the ratio of the *Dhfr* gene copy number to the 18S rRNA reference gene copy number. The amplification of the *Dhfr* gene was calculated relative to the *Dhfr* gene copy number of an untreated 3T6 cell line.

### **Assay of NQO1 Enzyme Activity.**

DT-D was assayed as dicoumarol-inhibitable NAD(P)H: dichlorophenolindophenol reductase essentially as described by Hodnick and Sartorelli (16). Equal numbers of exponentially growing AH13r cells were removed from the medium by centrifugation and resuspended in 1 ml of ice-cold PBS. Cells were kept on ice and homogenized twice for 30 s with an Ultra-Turrax T8 homogenizer (IKA, Staufen, Germany). Dicoumarol-sensitive NADPH:2,6-dichloroindophenol (DCPIP) reductase was assayed in a reaction mixture containing 0.05 M potassium phosphate (pH 7.5), 0.3 mM NADPH, 0.04 mM DCPIP, 0.07% BSA, and 0.1 ml of homogenized cells in a final volume of 1 ml. The reaction was initiated by the addition of NADPH, and the rate of DCPIP reduction was determined at a wavelength of 600 nm. Dicoumarol (1 µM final concentration) was then added, and the rate was measured again. The rate of dicoumarol-sensitive NADPH:DCPIP reductase was determined as the difference between the uninhibited and dicoumarol-inhibited rates.

### **Two-Dimensional Gel Electrophoresis.**



AH13r cells were treated for 17 days (36 h recovery for samples 5 and 6) as follows: (a) DMSO (untreated control); (b) BVDU; (c) MMC; (d) MMC + BVDU; (e) recovery after MMC treatment; and (f) recovery with BVDU after MMC + BVDU treatment. Proteins of each group were separated by two-dimensional gel electrophoresis. Differentially expressed proteins were identified by MALDI-MS.



## Results

### ***In Vitro*** Experiments.

We first investigated 3T6 cells treated with increasing doses of MTX  $\pm$  BVDU. 3T6 cells were chosen because of their ability to amplify the *Dhfr* gene forming double minutes during treatment with MTX (17). BVDU inhibited induction of *Dhfr* amplification. Whereas treatment with MTX induced amplification of *Dhfr* to give 4–27 copies (mean 14) after 39 days, cells cotreated with 10  $\mu$ g/ml BVDU amplified the *Dhfr* gene only 3–7 times (mean 4). Additional treatment sustained this effect (Fig. 1A).





Fig. 1. *In vitro* experiments. A, *Dhfr* gene amplification in mouse 3T6 cells (nine independent sublines each). B, effect of BVDU on cell numbers and apoptosis in AH13r rat sarcoma cells. *Left*, treatment with cytostatic drugs only, or in combination with BVDU (three independent experiments). DOX, 1.33 ng/ml; MXA, day 0: 0.1 ng/ml, day 2: 0.1 ng/ml, day 5: 0.1 ng/ml, day 8: 0.15 ng/ml; MMC, day 0: 35 ng/ml, day 4: 50 ng/ml, day 8: 75 ng/ml; 10 µg/ml BVDU. *Right*, HOPI stain evaluation (mean value ± SD, nine independent experiments). C, effect of BVDU on the recovery of AH13r cells (three independent experiments).

Furthermore, BVDU cotreatment sensitized AH13r sarcoma cells for chemotherapy-induced apoptosis (Fig. 1B). BVDU cotreatment significantly reduced cell numbers. BVDU itself was nontoxic (data not shown). We detected increasing numbers of pyknotic cells (7.5–11.5 µm diameter) as a result of BVDU combinatorial treatment (Fig. 2A). This observation indicated an induction of apoptosis.

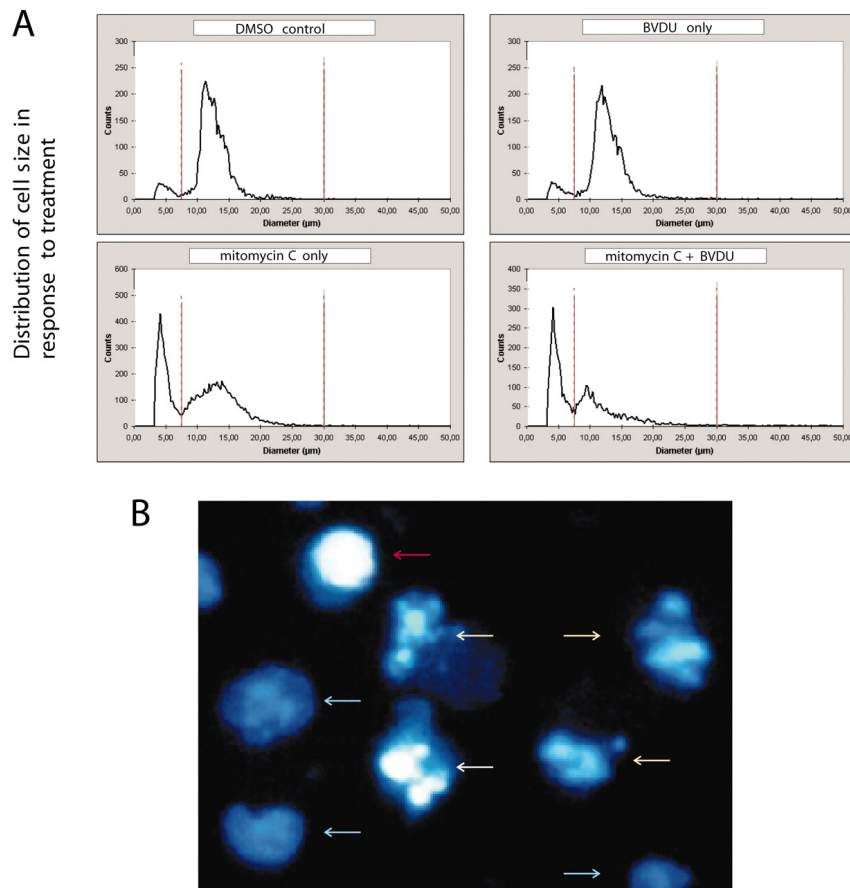




Fig. 2. Assessment of apoptosis. *A*, treatment of AH13r rat sarcoma cells. Cell size distribution profiles obtained on day 14 of MMC treatment, using the CASY Cell Counter and Analyzer. AH13r cells were treated with 0.05% DMSO (*control*), 10 µg/ml BVDU, increasing doses of 35–75 ng/ml MMC only, and MMC+BVDU. *B*, apoptosis assay. HOPI staining image, example. *Blue arrows*, viable cells; *yellow arrows*, early apoptosis; *white arrow*, late apoptosis; *red arrow*, necrosis.

These results were confirmed by HOPI analysis (10) ; Fig. 2*B*). BVDU cotreatment increased the number of apoptotic cells on average by 15% (Fig. 1*B*, *right*).

We next investigated several survival pathways using Westernblot analysis. This included the Akt/forkhead-related transcriptionfactor pathway, the Raf/extracellular signal-regulated kinase, MDM2, p14, p53, p38, and survivin pathways. Neither of those appeared to be affected by BVDU cotreatment. Also, the expression patterns of several cell cycle regulators such as p27, p16, cyclin-dependent kinases, and cyclins remained unchanged (data not shown).

However, BVDU in combination, but not by itself, reduced the amount of the oncogene protein STAT3 to up to 50% (Fig. 3*A*). Moreover, in combination with DOX or MMC, this reduction of STAT3 expression by BVDU was maximal during recovery, when the cytostatic drug was omitted after previous treatment, but BVDU was still present (see Fig. 1*C*). Additionally, during MMC recovery, the oncogene protein JUN-D was overexpressed, but remained at control level in the presence of BVDU. Treatment was also accompanied by activation of caspase-3 (Fig. 3*A*).

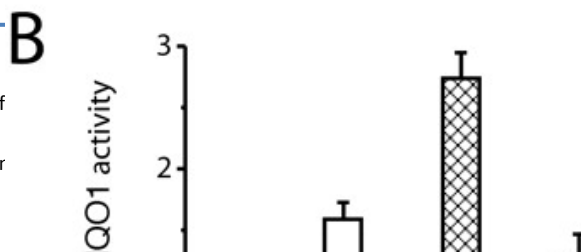
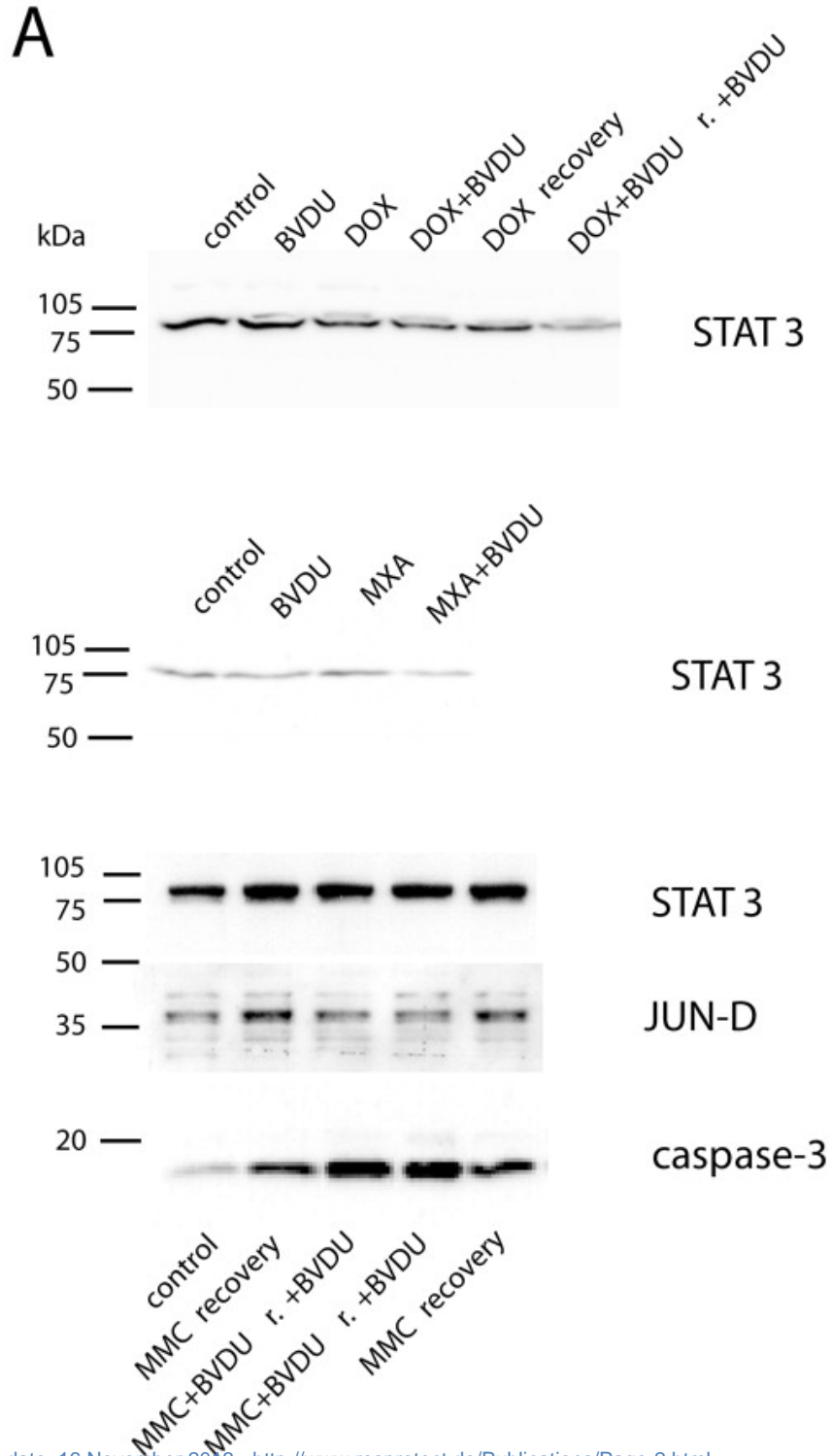




Fig. 3. Effect of BVDU combinatorial treatment on protein expression. A, Western blot analysis, expression of STAT3, JUN-D, and caspase-3 (proteolytically activated form) in response to cytostatic drug treatment. The expression levels were determined densitometrically (*r.* = recovery, see Fig. 1C). B, NQO1 enzyme activity (mean value ± SD, six independent experiments).

We investigated NQO1 activity in cell extracts (16) after treatment with the cytostatic drugs ± BVDU (Fig. 3B). BVDU cotreated cells showed higher NQO1 activity than untreated control cells or cells treated with cytostatic drugs only. Interestingly, cells treated with MMC+BVDU, which caused the strongest antiproliferative effect, did not enhance NQO1 activity. To elucidate the effects of BVDU, we performed a two-dimensional gel electrophoresis and identified differentially expressed proteins by MALDI-MS (Table 1). During combinatorial MMC+BVDU treatment, or during recovery (MMC omitted, BVDU present) from combinatorial treatment, the expression of three major "clusters" of protein classes was affected: (a) microfilamental (or regulatory) proteins were up-regulated during recovery (actins, tubulin, myosin, and tropo-modulin); (b) proteins involved in ATP generation were down-regulated (succinate dehydrogenase, pyruvate dehydrogenase, and malic enzyme; however, malate dehydrogenase was up-regulated); and (c) proteins regulating DNA repair were suppressed (APEX and UBE2N). One protein with oncogenic potential, DDX1, was affected by BVDU alone. In total,

75% of the spots were identified by MALDI-MS.

Table 1 Effects of cotreatment of MMC with BVDU on protein expression

Proteins	Fold change	MMC	BVDU	MMC+BVDU
DDX1	1.5	+	+	+
Actin	1.2	-	-	+
Tubulin	1.2	-	-	+
Myosin	1.2	-	-	+
Succinate dehydrogenase	0.8	-	-	-
Pyruvate dehydrogenase	0.8	-	-	-
Malic enzyme	0.8	-	-	-
Malate dehydrogenase	1.5	-	-	+
APEX	0.5	-	-	-
UBE2N	0.5	-	-	-



***In Vivo*** Experiments.

*In vivo*, BVDU enhanced anticarcinogenic effects on AH13r sarcomasin rats. Three cytostatic drugs of different mode of action (DOX, glufosfamide, and cisplatin) were tested in two independent experiments (Fig. 4A, panels 1 and 3). On the basis of previous results with rats (17), we used a daily dose of 15 mg/kg to gain peak plasma levels of

25 µg/ml 20 min after application. After cotreatment, BVDU was additionally administered in the recovery phase for 4 days (Fig. 4)

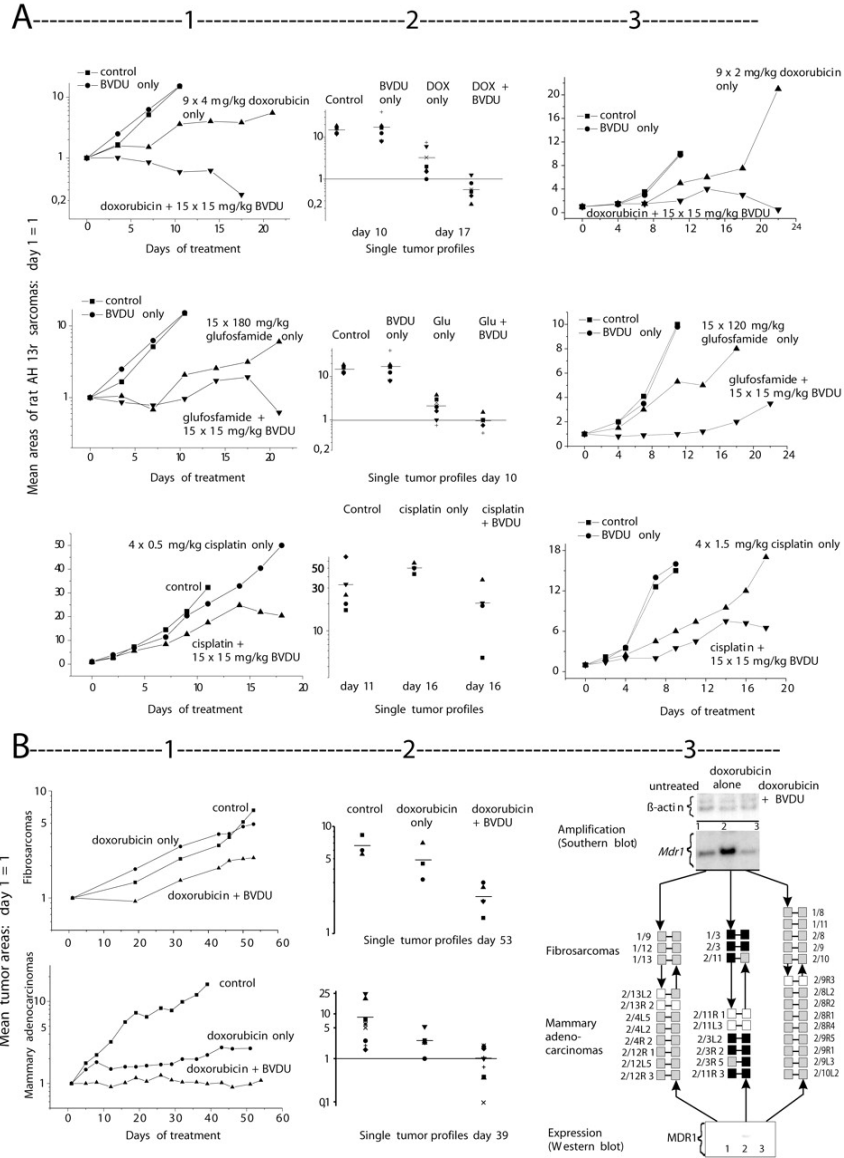


Fig. 4. SD-rats treated with DOX, glufosfamide, and cisplatin. A, rats with AH13r sarcomas. A1 and A3, comparison of control animals, BVDU-control animals, cytostatic drug-treated animals, and cytostatic drug+BVDU-treated animals (calculation of the mean of all individual tumor areas). A2, tumor areas of single tumors 10 and 17 days after treatment start (—mean). B, rats with DMBA-induced fibrosarcomas



and mammary adenocarcinomas. *B1, top*, SD-rats with DMBA-induced fibrosarcomas, calculation of the mean tumor area. Three control animals, three DOX-treated animals, and five DOX+BVDU-treated animals with fibrosarcomas. *Bottom*, DMBA-induced mammary adenocarcinomas, calculation of the mean of all individual tumor areas. Within the control animals, 8 tumors, within the DOX-treated animals, 6 tumors, and within the DOX+BVDU-treated animals, 9 tumors could be observed. *B2*, area of the individual tumors 39 days after treatment start (—mean). *B3*, *Mdr1* gene amplification and expression patterns of DMBA-induced fibrosarcomas and mammary adenocarcinomas in SD-rats. Representative tumor of 1) rat treated with solvent, 2) rat treated with DOX, and 3) rat treated with DOX+BVDU. Amplification of the *Mdr1* gene was detected by Southern blot analysis and expression of the MDR1 protein by Western blot analysis using the murine anti-P-glycoprotein monoclonal antibody JSB-1. The densitometrically determined *Mdr1* gene dosages (amplification levels) were subdivided into two categories.

 , indicate normal copy number,  
 , amplification.  
 , indicate that no analysis was performed because the whole tumor probe was used for histological analysis. Western blot analysis gave a yes (  
 ) or no (  
 ) result in respect to *Mdr11* = male, 2 = female/animal number, position of mammary adenocarcinomas). gene express patterns. The numbers indicate different tumors examined (1 male, 2 female/animal number, position of mammary adenocarcinomas).



The BVDU cotreated groups showed significantly less tumor growth. The tumor areas of these groups were significantly smaller than that of controls or the groups which were treated with cytostatic drugs only (Fig. 4A, *panel 2*), with the differences being significant at the 5% level (*t*-test/Mann-Whitney test). Whereas the treatment with cytostatic drugs (DOX, cisplatin, and navelbine+ifosfamide+cisplatin) led to a defined loss of body weight, cotreatment with BVDU partly inhibited loss of body weight (Table 2). This may indicate reduced nonspecific toxicity and optimized antitumor efficiency of the BVDU cotreatment. If cytostatic treatment led to a gain of body weight, BVDU cotreatment did not additionally support this effect.

Table 2 BVDU reduced unspecific toxic effects in cytostatic drug-treated rats (mean of the data of six to seven rats)

Treatment	Change of mean area of AH13r rat sarcomas (day 1 = 1) Day 14	Change of mean net body weight Day 14
BVDU 5 mg/kg cisplatin only	100%	100%



Interestingly, in AH13r tumors or tumor cells, we could neither observe gene amplification or genome-wide changes (data not shown). We used *in situ* CGH (18) and PCR to test for amplification of genes that are frequently amplified in tumors, *i.e.*  $\beta$ -actin (control), *ErbB2*, *Gstt1*, *Mdr1*, *c-Myc*, *n-Myc*, and topoisomerase IIa/GST-

0

1 encoding gene (*Top2a*).

In additional *in vivo* studies, BVDU cotreatment enforced growth retardation of DMBA-induced fibrosarcomas and mammary adenocarcinomas in SD-rats. The DMBA-induced fibrosarcoma growth of control animals surpassed the fibrosarcoma growth of the DOX-treated rats only at the end of the treatment period. In contrast, DOX+BVDU-treated animals showed an inhibited tumor growth over the whole time period analyzed (Fig. 3B, panel 1). When the areas of individual tumors were compared 53 days after treatment, the mean tumor area of the DOX+BVDU group was significantly smaller than that of the DOX or control group (Fig. 4B, panel 2).

We observed similar, but much more pronounced, effects with mammary adenocarcinomas (Fig. 4B, panel 1). DOX- (6 tumors) or DOX+BVDU-treated animals (9 tumors) showed an inhibited tumor growth over the whole treatment period in comparison with the control group (8 tumors). The areas of the individual tumors (Fig. 4B, panel 2) showed clear differences 39 days after treatment start. In 4 of 9 tumors of the DOX+BVDU group, a clear regression was observed. The overall tumor area of the DOX+BVDU group was significantly smaller than that of the DOX group or of controls. All of the differences were significant at the 5% level (*t*-test/Mann-Whitney test).

Tumors of rats treated with DOX showed amplification and/or overexpression of the *Mdr1* gene, whereas tumors of DOX+BVDU-treated or control rats showed neither amplification nor overexpression (Fig. 4B, panel 3).



## Discussion

Our results indicated that BVDU cotreatment enhanced chemosensitivity. This might have been because of: (a) inhibition of oncogenic and DNA repair-associated enzymes; (b) induction of NQO1 activity; (c) suppression of chemotherapy-induced *Mdr1* or *Dhfr* gene amplification; or (d) inhibition of the overexpression of survival pathways and reduced expression of ATP-generating enzymes in the recovery phase.

Three rat tumor models gave evidence that BVDU cotreatment contributed significantly to tumor regression *in vivo*.

DDX1, which was down-regulated by BVDU alone, seems to be of special importance. *DDX1* is coamplified with *MYCN* and overexpressed in a subset of neuroblastoma and retinoblastoma cell lines/tumors (20,21). Preliminary studies have shown that neuroblastoma patients with amplification of both *DDX1* and *MYCN* have a worse prognosis than patients with only the *MYCN* gene amplified (21). Thus, *DDX1* seems to have oncogenic potential, and it is predicted to function by RNA binding and modulation of RNA secondary structure.

Of the five genes affected by BVDU cotreatment with MMC, two are linked to DNA repair. BVDU reduced the expression of *UBE2N* and *APEX* to

30% of control level. The *UBE2N* gene encodes a ubiquitin-conjugating enzyme, which is thought to be involved in protein degradation. The protein complex containing *UBE2N* seems to be involved in the assembly of novel polyubiquitin chains for signaling in DNA repair and, through differential ubiquitination of PCNA, affects resistance to DNA damage (22,23).

Apurinic sites result from treatment with cytostatic drugs. The resulting abasic sites can block the progress of the DNA replication apparatus. These sites must be corrected to restore genetic integrity. Silencing of *APEX* expression by RNA interference nearly doubled specific cell lysis, showing enhanced DNA nicking (24).

BVDU induced NQO1. This is in accordance with the observation that a multifactorial multidrug resistance phenotype of tumor cells involves a decrease and not an increase in NQO1 expression (9). NQO1 enzyme activity was enhanced in response to BVDU combinatorial treatment with DOX or MXA, respectively. Hence, it can be speculated that enforced NQO1-mediated bioactivation of DOX and MXA could increase the cytotoxic potential of these drugs. On the other hand, MMC, its effects being strongest depending on NQO1 enzyme activity, showed no enhancement of NQO1 activity. Therefore, the sensitizing effect of BVDU does not seem to be implicitly NQO1-dependent.

Many of the drugs used in anticancer therapy, such as DOX and MXA (25), perturb the redox state and the mitochondrial respiration of the target cancer cell, which leads to the production of ROS. However, a



subsequent burst of ROS will indiscriminately affect not only tumor cells but also normal tissue, which causes unwanted systemic side effects during therapy. NQO1 is a scavenger of ROS, and that way, induced NQO1 activity can protect cells from nonspecific ROS and electrophile attack (26). This may explain the improved therapeutic outcome against experimental tumors *in vivo* with no systemic toxicity and gain of body weight in response to BVDU cotreatment, as was observed in our animal models.

The first direct evidence that in some tumor cells overexpression of genes because of amplification gives cells a selective advantage in the presence of a cytostatic drug derives from analysis of tumor cells taken from patients treated with MTX, an inhibitor of the enzyme DHFR (1). Resistance to MTX in human tumors has in many cases been shown to be associated with amplification of the gene encoding DHFR (27). Furthermore, expression of the *DHFR* gene has been implicated in resistance to a variety of chemotherapeutic agents and has been detected in human ovarian and colon tumors (28).

In our experiments, treatment with DOX for 50 days caused *Mdr1* gene amplification and overexpression in DMBA-induced rat tumors. Cotreatment with BVDU inhibited this cytostatic drug-induced effect. Beyond that, *Dhfr* gene amplification was inhibited in 3T6 mouse cells.

A comprehensive effect of BVDU was observed in the recovery phase. Gene products linked to survival, microfilament formation, differentiation, signal transduction, and ATP generation were affected.

BVDU inhibited survival pathways and enforced apoptotic response. BVDU cotreatment might have promoted apoptosis by blocking an antiapoptotic survival pathway involving STAT3 and JUN-D. Additional mechanisms are quite likely, but still under investigation.

Constitutively activated STAT3 is oncogenic (7) and contributes to the development of various human cancers (29) by inhibiting apoptosis (30). Thus, STAT3 promotes cell survival and renders cancer cells resistant to chemotherapy. Accordingly, the inhibition of STAT3-signaling induces apoptosis specifically in tumor cells, and increases sensitivity to chemotherapeutic agents (7). Along this line, it was demonstrated that dominant-negative *Stat3*-expression sensitizes melanoma cells to FAS-L-induced apoptosis (30). Therefore, STAT3-signaling in human tumors has been proposed as a novel molecular target for therapeutic intervention to reduce resistance of tumor cells to apoptosis (29). JUN-D is an essential and ubiquitously expressed component of the activating protein-1 transcription factor complex. *Jun-D(-/-)* primary fibroblasts exhibit premature senescence and increased sensitivity to p53-dependent apoptosis on UV-irradiation or tumor necrosis factor

treatment (8), which suggests that JUN-D may activate the nuclear factor

B survival pathway. Moreover, p202, which is directly regulated by JUN-D, renders fibroblasts more refractory to apoptosis (31). In support of this reasoning, we demonstrated that BVDU cotreatment down-regulated the STAT3 and JUN-D survival pathways, thereby limiting chemoresistance.



## Acknowledgments

We thank Clemens Dasenbrock (Hannover, Germany) for supervising the *in vivo* experiments and Volker Rehse (Hannover, Germany) for performing them. Furthermore, we thank Christian Scheler, Proteome Factory (Berlin, Germany) for performance of the two-dimensional gel-electrophoresis and protein identification by MALDI-MS.

## Footnotes

The costs of publication of this article were defrayed in part by the payment of page charges. This article must therefore be hereby marked *advertisement* in accordance with 18 U.S.C. Section 1734 solely to indicate this fact.

1 Supported by the "Sächsische Aufbaubank" (Dresden/Germany) Project 6261, and the Fraunhofer-Society (München/Germany).

2 To whom requests for reprints should be addressed, at RESprotect, Fiedlerstr. 34, D-01307 Dresden, Germany. Phone: +493514503201; Fax: +493514503210; E-mail: [fahrig@resprotect.de](mailto:fahrig@resprotect.de).

1)

2)

3)

4)

5)

6)

7)

8)

9)

10)

11)



12)

13)

14)

15)

16)

17)

18)

19)

20)

21)

22)

23)

24)

25)

26)

27)

28)

29)

30)

31)